Journal of Nuclear Medicine, published on November 10, 2022 as doi:10.2967/jnumed.122.264816

Cure of disseminated human lymphoma with [^{177}Lu]Lu-ofatumumab in a preclinical model

Kyuhwan Shim[1*], Mark S. Longtine[1*], Diane S. Abou[1], Mark J. Hoegger[1], Richard S. Laforest[1], Daniel L. J. Thorek[1,2], and Richard L. Wahl[1,3]

[1]Mallinckrodt Institute of Radiology, Washington University School of Medicine, St. Louis, MO, 63110

[2]Department of Biomedical Engineering, Washington University, St. Louis, MO

[3]Department of Radiation Oncology, Washington University, St. Louis, MO

*Contributed equally to this work

Corresponding author: Richard Wahl, Mallinckrodt Institute of Radiology, 510 South Kingshighway Blvd, St. Louis, MO 63110. mlongtine@wustl.edu, 314-362-7100

First Author: Kyuhwan Shim, Mallinckrodt Institute of Radiology, Washington University School of Medicine, St. Louis, MO

Running Title:

[^{177}Lu]Lu-ofatumumab lymphoma therapy

Disclosure:

RLW, scientific advisory board and stock options: Clarity Pharmaceuticals, Voximetry. Scientific advisory board: Seno Medical. Honoraria: Bristol Myers Squibb, Actinium Pharmaceuticals, Jubilant Draximage, ITM. Research support: Actinium Pharmaceuticals, BMS, Bayer, Siemens, White Rabbit AI. DA, DLJT has an advisory board role for and stock in Diaprost AB and Pharma15. RL is a consultant to Curium Pharmaceuticals. No other potential conflicts of interest relevant to this article exist.

Abbreviations:

^{177}Lu, Lutetium-177; TLC, thin-layer chromatography; FPLC, fast protein liquid chromatography; cpm, counts per minute; OD, optical density; % IA/g, percent injected activity per gram.

ABSTRACT

Although immunotherapies that target CD20 on most non-Hodgkin lymphoma (NHL) cells have improved patient outcomes, current therapies are inadequate as many patients are or become refractory or undergo relapse. Here, we label the third-generation human anti-CD20 antibody, ofatumumab, with lutetium-177 (^{177}Lu), determine the in vitro characteristics of [^{177}Lu]Lu-ofatumumab, estimate human dosimetry, and assay tumor targeting and therapeutic efficacy in a murine model of disseminated NHL.

Methods: CHX-A"-DTPA-[^{177}Lu]Lu-ofatumumab was prepared. We evaluated radiochemical yield, purity, in vitro immunoreactivity, stability, (n=7), affinity, and killing of CD20-expressing Raji cells (n=3). Human dosimetry was estimated from biodistribution studies as % injected activity per gram (% IA/g) using C57Bl/6N mice. Tissue/organ biodistribution was determined in R2G2 immunodeficient mice with subcutaneous Raji-cell tumors. Therapy studies used R2G2 mice with disseminated human Raji-luc tumor cells (n=10 mice/group). Four d post cell injection, mice were untreated or treated with ofatumumab, 8.51 MBq of [^{177}Lu]Lu-IgG or 0.74 or 8.51 MBq of [^{177}Lu]Lu-ofatumumab. Survival, weight, and bioluminescence were tracked.

Results: Radiochemical yields were 93±2%, radiochemical purities 99±1% and specific activities 401±17 MBq/mg. Immunoreactivity was substantially preserved and >75% ^{177}Lu remained chelated after 7 d in serum. [^{177}Lu]Lu-ofatumumab specifically killed Raji-luc cells in vitro (p<0.05). Dosimetry estimated an effective dose for human administration of 0.36 mSv/MBq and that marrow may be the dose-limiting organ. Biodistribution in subcutaneous tumors 1, 3 and 7 after [^{177}Lu]Lu-ofatumumab injection

was 11, 15, and 14% IA/g, respectively. In the therapy study, median survival of untreated mice was 19 d, not statistically different than mice treated with 8.51 MBq of [^{177}Lu]Lu-IgG (25 d). Unlabeled ofatumumab increased survival to 46 d, similar to 0.74 MBq of [^{177}Lu]Lu-ofatumumab (59 d), with both superior to no treatment (p<0.0003). Weight loss and increased tumor burden preceded death or sacrifice for cause. In contrast, treatment with 8.51 MBq of [^{177}Lu]Lu-ofatumumab dramatically increased median survival (>221 d), permitted weight gain, eliminated detectable tumors, and was curative in 9/10 mice.

Conclusion: [^{177}Lu]Lu-ofatumumab shows favorable in vitro characteristics, localizes to tumor, and shows curative therapeutic efficacy in a disseminated lymphoma model, showing potential for clinical translation to treat NHL.

Key Words: CD20; lymphoma; targeted beta-particle therapy; radioimmunotherapy; lutetium

INTRODUCTION

Non-Hodgkin lymphoma (NHL) is a common hematological malignancy, with over 80,000 new cases and 20,000 deaths estimated for the US in 2022 *(1)*. The standard of care for many NHL involves chemotherapy and immunotherapy targeting the CD20 protein that is highly expressed on most NHL cells, with murine/human chimeric rituximab used most commonly. Although this chemotherapy with immunotherapy combination is usually initially effective, many patients are refractory or undergo relapse, indicating the need for improved therapies.

Radioimmunotherapy joined clinical practice two decades ago with Food and Drug Administration approval of two anti-CD20 radioimmunotherapies for lymphoma: Zevalin® ([^{90}Y]Y-ibritumomab tiuxetan) and Bexxar® (tositumomab and ^{131}I-tositumomab), which use murine-derived antibodies radiolabeled with β-particle emitting radioisotopes. Because of potential immune reactions, these antibodies were approved for only a single therapeutic dose. ^{90}Y ($t_{1/2}$ 2.7 d) emits high-energy β particles (934 keV_{ave}) while ^{131}I emits lower-energy β particles (187 keV_{ave}) with ranges in tissue of 3800 μm_{ave} and 360 μm_{ave}, respectively *(2)*, enabling killing over many cell diameters. Thus, in addition to individual tumor cells, β particles may work against larger tumors, tumor-cell aggregates with imperfect antibody access and heterogeneous tumors, although with potential off-target damage. Despite long-term safety and clinical effectiveness, Bexxar has been discontinued in the US and Zevalin is applied infrequently *(3)*, in part due to economic and logistical concerns present when they were introduced and to competing non-radioactive therapies *(4)*.

Some concerns that limited the Bexxar and Zevalin utilization have been overcome with greater integration of radiopharmaceutical therapy into medicine *(5)*, as exemplified by the Food and Drug Administration approval of lutetium-177 (^{177}Lu)-labeled agents for prostate cancer treatment (Pluvicto®, *(6)* and neuroendocrine tumors (Lutathera®, *(7)*. ^{177}Lu ($t_{1/2}$ 6.6 d) emits β particles of 149 keV_{ave}, with a tissue range of 220 μm_{ave}. Emission of low abundance γ particles by ^{177}Lu permits imaging by SPECT.

Recently, ofatumumab, a third-generation anti-CD20 fully human antibody, has been developed. Ofatumumab is a Type I antibody that is internalized after CD20 binding *(8)*. We showed by biodistribution and PET imaging studies that [^{89}Zr]Zr-Dfo-ofatumumab targets CD20-positive subcutaneous xenograft tumors as well as [^{89}Zr]Zr-Dfo-rituximab *(9)*.

Here, we describe the synthesis and evaluation of [^{177}Lu]Lu-ofatumumab. We present in vitro characteristics, dosimetry estimation and subcutaneous tumor targeting. We also show that [^{177}Lu]Lu-ofatumumab therapy results in long-term survival and elimination of tumor cells in a murine model of disseminated human lymphoma.

MATERIALS AND METHODS

Reagents and Cell Culture

Ofatumumab (IgG1 kappa, Novartis) was purchased from the Washington University Clinical pharmacy and human IgG1 kappa from BioXcel. Raji cells and Raji-luc cells stably expressing luciferase *(10)* were cultured as described *(9)*. SCN-CHX-A**"**-DTPA was from Macrocyclics, size exclusion chromatography (SEC) columns from Fisher Scientific and D-Luciferin from GoldBio. Sigma provided human serum, sodium

acetate, diethylenetriamine pentaacetate, tetramethylammonium acetate and L-sodium ascorbate. ^{177}Lu from the University of Missouri was dissolved in 0.2 M HCl. SG thin-layer chromatography (TLC) paper was from Agilent and the MTS tetrazolium salt assay was from Promega.

Antibody Conjugation, Radiolabeling, Thin-layer Chromatography, Mass Spectrometry and FPLC

Antibody was incubated with SCN-CHX-A"-DTPA in 0.1 M pH 9.0 sodium carbonate at a chelator:antibody molar ratio of 8:1 for 1 h at 37˚C and purified by SEC into 0.5 M NH_4OAc pH 7.0. 477 MBq ^{177}Lu was added to 400 µg CHX-A"-DTPA-antibody with 20 mM NH_4OAc pH 7.0. After 2 h at 37˚C, DTPA was added to 5 mM followed by SEC purification into saline and the addition of 10 mg/mL L-sodium ascorbate. TLC and fast-performance liquid chromatography were done as described *(9)*. Radiochemical yield was assayed with a CRC55-tW dose calibrator. Chelate number was determined using a Fisher Scientific Exactive Plus EMR mass spectrometer operating at *m/z* 800-12000 Da and resolving power of 8750 or 17500 at 300 *m/z* with analysis using Protein Metric Intact software.

Serum Stability, Immunoreactivity, in vitro Stability, Affinity, and Cell Killing Assays

To assay stability, 14.8 MBq [^{177}Lu]Lu-ofatumumab or ^{177}Lu were added to 10% human serum in 20 mM NaOAc 150 mM NaCl pH 7.0 with 10 mg/mL L-SA or kept at 4˚C. At 0, 1, 5 and 7 d, aliquots were analyzed by TLC. Immunoreactivity was assayed as described *(9)*. To assay affinity, 2.5x10^6 Raji cells

without or with 10-µg ofatumumab were incubated with [^{177}Lu]Lu-ofatumumab, washed after 4 h at 23˚C and gamma counted. To assay cell killing, 2 x 10^6 Raji-luc cells in 1 mL RPMI medium with 10% heat-treated FBS were exposed to no treatment, ofatumumab, [^{177}Lu]Lu-IgG or [^{177}Lu]Lu-ofatumumab, with cognate unlabelled antibody added to 20 µg total. After 14 h at 37˚C, cells were washed and 20% were resuspended in fresh medium for an additional 168 h followed by MTS assay.

Biodistribution of [^{177}Lu]Lu-ofatumumab in Mice with Subcutaneous Raji Tumors

The Washington University in St. Louis Animal Care and Use Committee approved animal studies. Biodistribution with tumor-bearing mice used female 6-8-week-old immunodeficient Rag2-IL2rg (R2G2, B6;129-*Rag2*^{tm1Fwa}*Il2rg*^{tm1Rsky}/DwlHsd)) mice (Envigo) injected subcutaneously with 5x10^6 Raji-luc cells. Mice with palpable tumors were injected intravenously with 10-20 µg of [^{177}Lu]Lu-ofatumumab and sacrificed 1, 3 and 7 d later. Distribution was calculated as decay-corrected percent injected activity (%IA/g) per gram using a Beckman 8000 gamma counter and a 1-500 keV window.

Dosimetry Estimation

Naïve 5-6-week-old C57Bl6/N mice injected intravenously with 370 kBq (10 µg) of [^{177}Lu]Lu-ofatumumab were sacrificed 4 h and 1, 2, 5 and 11 d later and tissue/organs γ counted. Bone was counted after marrow separation. Urine and feces were collected at 4 h, 1 and 2 d. Organ residence times were calculated by analytical integration of single or multi-exponential fits of the time activity and scaled to human

organ weight by the "relative organ mass scaling" method *(11)*, which was not applied to the gastrointestinal tract organs. To estimate human radiation dose, residence times were entered into OLINDA v2.2 using the MIRD adult-female model and organ weights of the ICRP 106 *(12)*. The calculated radiation dose includes contributions from β and γ rays from ^{177}Lu within the organ, neighboring organs, and the remainder of the body.

Therapeutic Studies, Mouse Weight, and Bioluminescent Imaging

R2G2 mice (n=10 mice/group) injected intravenously with $1x10^6$ Raji-luc cells were left untreated or 4 d later were injected with ofatumumab, [^{177}Lu]Lu-IgG, or [^{177}Lu]Lu-ofatumumab. When used, 20 µg of antibody was injected/mouse. Bioluminescent images were acquired as described *(13)*. Mice were sacrificed for hind-limb paralysis, >20% weight loss, or other signs of morbidity.

Statistics

Statistical analyses used Prism 9.0 software (GraphPad). Tests are noted in the text or Figure Legends.

RESULTS

Synthesis of [^{177}Lu]Lu-ofatumumab and Radiochemical Yield, Purity, and Immunoreactivity

SCN-CHX-A”-DTPA was conjugated to ofatumumab and purified. Mass spectrometry indicated an average of 3.2 chelators per antibody. After ^{177}Lu radiolabeling, [^{177}Lu]Lu-ofatumumab was purified (n=7). Radiochemical purity was

>99±1%, radiochemical yields were 93±2%, and specific activities were 401±17 MBq/mg. Immunoreactivity was 49±3% and 2±1% after blocking with unlabeled ofatumumab.

Serum Stability, In Vitro Cell Killing and Affinity of [^{177}Lu]Lu-ofatumumab

After 7 d, over 90% of ^{177}Lu remained chelated in buffer at 4˚C and over 75% in human serum at 37˚C (Supplemental Fig. 1A). Targeting and killing of CD20-expressing cells was assayed (Supplemental Fig. 1B) by adding no antibody or 0.74 to 11.10 MBq/mL of [^{177}Lu]Lu-ofatumumab or [^{177}Lu]Lu-IgG to Raji-luc cells, incubated 14 h, media changed, and cell viability determined 168 h later. Compared to no antibody, [^{177}Lu]Lu-IgG showed no cell killing at any dose. [^{177}Lu]Lu-ofatumumab at 3.7 MBq/mL and higher showed dose-dependent killing compared to no antibody and [^{177}Lu]Lu-IgG (p<0.05, n=3). [^{177}Lu]Lu-ofatumumab showed a 4.3 nM K_d for CD20 (Supplemental Fig. 1C), consistent with that noted previously (see 2F2 in *(14)*).

Biodistribution of [^{177}Lu]Lu-ofatumumab in C57Bl6/N Mice and Estimation of Human Dosimetry

[^{177}Lu]Lu-ofatumumab biodistribution was determined in C57Bl6/N mice 4 h and 1, 2, 7 and 11 d post injection (Supplemental Table 1) as percent of injected activity per gram (% IA/g). Blood % IA/g was 38% at 4 h and 19% after 11 d. Bone distribution was <4%, indicating stable chelation as free ^{177}Lu is a bone-seeking radionuclide *(15)*. Liver was 9% at 4 h and 5% IA/g at 11 d and marrow 14% at 4 h and 9% IA/g at 11 d. Spleen was 8-9% IA/g. Approximately 13% of the injected activity was excreted.

To estimate human dosimetry, integrated time-activities for [^{177}Lu]Lu-ofatumumab were calculated (Supplemental Table 2). The longest (59.7 h) was in the blood with extended time-activities seen in the blood-rich heart cavity, lung and liver. Due to its large mass, muscle time-activity was second at 39 h. The adult human female model (Table 1) showed estimated dosimetry of 0.2-0.5 mSv/MBq in most organs, with the largest to heart wall (1.02 mSv/MBq), with liver, spleen and kidney doses of 0.36, 0.48, and 0.43 mSv/MBq, respectively. Estimated doses to the osteogenic cells (bone surfaces) and red marrow are 0.82 and 0.54 mSv/MBq, respectively. The estimated effective dose is 0.36 mSv/MBq.

Biodistribution of [^{177}Lu]Lu-ofatumumab in Mice with Subcutaneous Raji-cell Tumors

Biodistribution was investigated in R2G2 mice with subcutaneous Raji-cell tumors (Fig. 1). These mice are proficient in double-strand DNA-break repair and are less likely to show artifactual radiation toxicity than repair-deficient *Prkdc*^{SCID} mice *(16)*. [^{177}Lu]Lu-ofatumumab was injected at a low activity (370-444 kBq) to limit therapeutic effect and biodistribution determined 1, 3 and 7 d later (n=3-16 mice/time point). Blood decreased from ~13 to 6% IA/g with similar splenic distribution. Liver levels were ~5% and marrow was 10% at 1 d and 5% IA/g at 7 d. Bone distribution was 2-3% IA/g. Tumor targeting was 11%, 15% and 14% IA/g at 1, 3 and 7 d, respectively.

Murine Therapy Study

To evaluate [^{177}Lu]Lu-ofatumumab therapeutic efficacy, R2G2 mice were injected intravenously with Raji-luc cells and tumor-cells quantified by bioluminescent imaging

(13). After injection, these cells disseminate to many organs *(10,13,17,18)*, with hind-limb paralysis a typical cause for sacrifice due to growth in and around the spine.

Four d after cell injection, mice were untreated, treated with native ofatumumab, 8.51 MBq [^{177}Lu]Lu-human IgG1 or with 0.74 MBq (30±2.2 MBq/kg) or 8.51 MBq (345±25.1 MBq/kg) of [^{177}Lu]Lu-ofatumumab (n=10 mice/group). Survival (Fig. 2), weight (Supplemental Fig. 2) and bioluminescence (Fig. 3A) were tracked for 221 d. Representative bioluminescent images at selected time points shown in Fig. 3B and images of all mice just prior to death or sacrifice for cause or study termination are shown in Fig. 4.

The median survival of untreated mice was 19 d with none surviving beyond 22 d. Unlabeled ofatumumab yielded median survival of 46 d, superior to untreated mice (Mantel-Cox, p<0.0001), with one mouse surviving without weight loss or increased bioluminescence. 8.51 MBq of [^{177}Lu]Lu-IgG yielded 0/10 surviving mice and a median survival of 25 d, which was not different from that of untreated mice. For all three groups, increased bioluminescence and weight loss occurred prior to death or sacrifice for cause.

0.74 MB of [^{177}Lu]Lu-ofatumumab yielded median survival of 59 d and 9/10 mice not surviving, with increased bioluminescence and weight loss prior to death or sacrifice for cause. This survival was superior to untreated mice (Mantel-Cox, p<0.0001) but not to unlabeled ofatumumab-treated mice. Hind-limb paralysis was frequently associated with death or sacrifice for cause (Supplemental Table 3).

Notable therapeutic efficacy resulted from 8.51 MBq [^{177}Lu]Lu-ofatumumab treatment, with 9/10 mice surviving with continuous low bioluminescence (Figs. 3, 4).

This survival was greater than that of untreated mice and of mice treated with unlabeled ofatumumab, 8.51 MBq [^{177}Lu]Lu-IgG or 0.74 MBq [^{177}Lu]Lu-ofatumumab (Mantel-Cox, p<0.0003 for all comparisons). One mouse succumbed at 117 d, but this appeared unrelated to tumor burden or therapy as no weight loss or increased bioluminescence occurred. Surviving mice displayed weight loss from 10 to 35 d post cell injection but recovered and gained weight.

To determine how quickly therapy affected tumor cells, bioluminescence slopes from 1 to 18 d post-initiation of therapy were compared (Fig. 5, Supplemental Fig. 3). Compared to no treatment, ofatumumab, 8.51 MBq [^{177}Lu]Lu-IgG and 0.74 MBq [^{177}Lu]Lu-ofatumumab slowed, but did not eliminate, tumor-cell proliferation. In contrast, 8.51 MBq [^{177}Lu]Lu-ofatumumab quickly eliminated tumor-cells, which was significant compared to untreated mice, treatment with unlabeled ofatumumab, 8.51 MBq [^{177}Lu]Lu-IgG or 0.75 MBq [^{177}Lu]Lu-ofatumumab (p<0.05).

DISCUSSION

Our preclinical studies add to prior work demonstrating the potential of radiolabeled anti-CD20 antibodies to treat NHL. We show that [^{177}Lu]Lu-ofatumumab can be produced with high radiochemical yields and purity, excellent affinity, and with good stability, immunoreactivity and potent cell killing. Additional advances include using a fully human anti-CD20 and ^{177}Lu, which has broad applicability in radiotherapy of cancer. We evaluated [^{177}Lu]Lu-ofatumumab therapy in a rapidly progressing disease model with dose-response studies and bioluminescence monitoring of tumor-cell burden. A single 8.51 MBq dose [^{177}Lu]Lu-ofatumumab displayed curative efficacy.

Human dosimetry estimates predict the highest dose from [^{177}Lu]Lu-ofatumumab (1.02 mSv/MBq) to the heart wall. The relatively radiation-resistant liver and spleen showed 0.36 and 0.48 mSv/MBq, respectively. The predicted dose to red marrow is 0.54 mSv/MBq and hematological toxicity likely will be dose limiting in clinical use, as was found with Bexxar, Zevalin, [^{177}Lu]Lu-J591 *(19)*, [^{177}Lu]Lu-G250 anti-CAIX *(20)* and [^{177}Lu]Lu-rituximab *(21)*. As 2 Sv is a typical maximal dose for acceptable hematologic toxicity without stem cell support, delivering this radiation to the marrow would be tolerable. As there may be patient-to-patient variability with [^{177}Lu]Lu-ofatumumab due to cross reactivity with normal CD20-positive cells, our dosimetry data provide guidance for activity administration to humans. Dosimetric estimation could also potentially be obtained using a PET imaging surrogate, such as [^{89}Zr]Zr-ofatumumab *(9,22)*.

The stable in vivo chelation of ^{177}Lu by CHX-A"-DTPA-ofatumumab agrees with the results of others using this chelator-radionuclide combination *(23,24)*. Although it has been suggested that macrocyclic DOTA requires high temperatures for stable ^{177}Lu chelation incompatible with maintaining antibody function *(24,25)*, experiments show this is not the case *(26,27*). Thus, CHX-A"-DTPA and DOTA both appear practical for chelation of ^{177}Lu to antibodies and antibody fragments.

Others have used [^{177}Lu]Lu-anti-CD20 intact antibodies or ^{177}Lu-labeled antibody-based radiopharmaceuticals for preclinical and clinical therapy. Ertveld et al. *(23)*, using a single-domain anti-CD20 antibody in immunocompetent mice with CD20-expressing subcutaneous tumors, found modest therapeutic effect at 140 MBq/mouse. 50 MBq/mouse induced expression of proinflammatory genes while 140 MBq/mouse increased the percentage in the tumor of PD-L1 positive myeloid cells and alternatively

activated macrophages. Krasniqi et al. *(28)* compared a single-domain anti-CD20 antibody with unlabeled rituximab and [^{177}Lu]Lu-CHX-A"-DTPA-rituximab in mice with CD20-expressing subcutaneous tumors. All treatments increased survival over no treatment but [^{177}Lu]Lu-CHX-A"-DTPA-rituximab was only slightly better than rituximab. In a phase I/II study of [^{177}Lu]Lu-DOTA-rituximab in 31 patients with relapsed or refractory CD20-positive lymphoma, mainly hematologic toxicity was observed with frequent tumor responses and 8/11 patients with follicular lymphoma alive after an 84-month median follow-up *(29)*.

A major finding of the current study is the high therapeutic efficacy of [^{177}Lu]Lu-ofatumumab in a murine model of disseminated lymphoma. Therapy was initiated 4 d post intravenous cell injection, when tumor cells are present individually or as small groups, comparable to micrometastatic or minimal residual disease in humans. 8.51 MBq of [^{177}Lu]Lu-ofatumumab reduced tumor burden within ~2 d and eliminated bioluminescence-detectable tumors, with 9/10 mice surviving 221 d later. This response was dose-dependent and specific as 0.74 MBq [^{177}Lu]-Lu ofatumumab and 8.51 MBq [^{177}Lu]-IgG did not extend survival or prevent tumor-cell proliferation. Although attenuation from tissue, skin and fur means bioluminescent imaging may not detect low tumor-cell burden *(13)*, the durability of the response suggests complete elimination of tumor cells by 8.51 MBq [^{177}Lu]Lu-ofatumumab. After initial weight loss, these mice gained weight, suggesting no or low whole-body toxicity. The internalization of ofatumumab after CD20 binding *(30)* and the residualization of ^{177}Lu within the cell may contribute to its therapeutic efficacy. Moreover, the lack of murine sequences in [^{177}Lu]Lu-ofatumumab suggests a potential for fractionated therapy or repeated

treatments. In an interesting approach, with relatively small subcutaneous tumors of rituximab-resistant Raji cells, Malenge et al. *(26)* combined [^{177}Lu]Lu-lilotomab (anti-CD37) and unlabeled rituximab, with good therapeutic results.

α-particle therapy is another potential approach to treat lymphoma. Using a murine Raji-cell disseminated lymphoma model, [^{213}Bi]Bi-rituximab (t½ 45.6min) was typically curative when tumor burden was low (4 d post-cell injection) but not when it was higher *(18)*, perhaps due to lack of time to target larger tumor masses before decay. Similarly, [^{149}Tb]Tb-rituximab (t½ 4.2 h) therapy initiated 2 d after Daudi-cell intravenous injection increased survival *(31)*. A 1F5 anti-CD20 antibody with chelated ^{211}At (t½ 7.2 h) was 80% curative when injected 6 d after intravenous cell injection, with supporting stem cell transplant, but only slowly reduced the growth of subcutaneous tumors *(32)*. Based on these results and on the multi-day tumor-targeting pharmacokinetics of intact antibodies, radioimmunotherapy of larger tumor masses with intact antibodies will likely be most successful using radioisotopes that permit tumor localization prior to decay, including ^{177}Lu or α-particle-emitting ^{225}Ac with its 10-d half-life.

Our studies add to the literature demonstrating the effectiveness of ^{177}Lu-radiopharmaceuticals in cancer therapy. We found remarkable effectiveness in micrometastatic disease and the 6.6-d half-life and multi-cell-diameter killing range of ^{177}Lu suggests [^{177}Lu]Lu-ofatumumab could be effective against larger tumors.

Although initial anti-CD20 radioimmunotherapies showed limited commercial success for several reasons, we suggest that a re-evaluation of next-generation β- and α-particle therapies is in order. [^{177}Lu]Lu-ofatumumab CD20-targeted

radioimmunotherapy may be an effective approach for therapy of non-Hodgkin lymphoma or other CD20-expressing diseases.

FUNDING

This study was supported in part by National Institutes of Health R01CA240711 (DLJT), R01CA229893 (DJLT), R01CA201035 (DLJT) and the Children's Discovery Institute MC-II-2021-961 (DA) and the NIGMS 5P41GM103422 to the Washington University Biomedical Mass Spectrometry Resource.

CONCLUSION

Chx-A"-DTPA-ofatumumab stably chelates ^{177}Lu in vitro and in vivo and [^{177}Lu]Lu-Chx-A"-ofatumumab effectively targets CD20-expressing tumor xenografts. In a mouse model of disseminated human lymphoma, therapy with [^{177}Lu]Lu-ofatumumab showed curative therapeutic efficacy.

ACKNOWLEDGMENTS

We appreciate the assistance of the Washington University Small Animal Imaging Core and cyclotron facilities.

KEY POINTS

QUESTION: Can [^{177}Lu]Lu-anti-CD20 ofatumumab be produced and effectively treat disseminated human non-Hodgkin lymphoma in a murine model?

PERTINENT FINDINGS: [^{177}Lu]Lu-ofatumumab specifically killed lymphoma cells in vitro, was cytotoxic in vivo as assessed by bioluminescence imaging, and was curative of disseminated human lymphoma in the murine model. Dosimetry estimates support the feasibility of human translation.

IMPLICATIONS FOR PATIENT CARE: [^{177}Lu]Lu-ofatumumab has exceptional potential for CD20-targeted radioimmunotherapy of patients with non-Hodgkin lymphoma.

REFERENCES

1. Siegel RL, Miller KD, Fuchs HE, Jemal A. Cancer statistics, 2022. *CA Cancer J Clin.* 2022;72:7-33.

2. Frost SH, Frayo SL, Miller BW, et al. Comparative efficacy of ^{177}Lu and ^{90}Y for anti-CD20 pretargeted radioimmunotherapy in murine lymphoma xenograft models. *PLoS One.* 2015;10:e0120561.

3. Shadman M, Li H, Rimsza L, Leonard JP, et al. Continued excellent outcomes in previously untreated patients with follicular lymphoma after treatment with CHOP plus rituximab or CHOP plus ^{131}I-tositumomab: Long-term follow-up of phase III randomized study SWOG-S0016. *J Clin Oncol.* 2018;36:697-703.

4. Sarbisheh EK, Price E. The radiopharmaceutical chemistry of the radioisotopes of lutetium and yttrium. In: Lewis JS, Windhorst AD, Zeglis BM, eds. *Radiopharm Chem*. 2019;359-370.

5. Wahl RL, Chareonthaitawee P, Clarke B, et al. Mars shot for nuclear medicine, molecular imaging, and molecularly targeted radiopharmaceutical therapy. *J Nucl Med.* 2021;62:6-14.

6. Hennrich U, Kopka K. Lutathera®: The first FDA- and EMA-approved radiopharmaceutical for peptide receptor radionuclide therapy. *Pharmaceuticals (Basel).* 2019;12:E114.

7. Keam SJ. Lutetium Lu 177 vipivotide tetraxetan: first approval. *Mol Diagn Ther.* 2022;26:467-475.

8. Klein C, Lammens A, Schafer W, et al. Epitope interactions of monoclonal antibodies targeting CD20 and their relationship to functional properties. *MAbs.* 2013;5:22-33.

9. Yoon JT, Longtine MS, Marquez-Nostra BV, Wahl RL. Evaluation of next-generation anti-CD20 antibodies labeled with ^{89}Zr in human lymphoma xenografts. *J Nucl Med.* 2018;59:121912-24.

10. Chao MP, Alizadeh AA, Tang C, et al. Anti-CD47 antibody synergizes with rituximab to promote phagocytosis and eradicate non-Hodgkin lymphoma. *Cell.* 2010;142:699-713.

11. Stabin M. Fundamentals of nuclear medicine dosimetry. New York, NY: Springer; 2008;77-119.

12. Radiation dose to patients from radiopharmaceuticals. Addendum 3 to ICRP Publication 53. ICRP Publication 106. Approved by the Commission in October 2007. *Ann ICRP.* 2008;38:1-197.

13. Hoegger MJ, Longtine MS, Shim K, Wahl RL. Bioluminescent tumor signal is mouse strain and pelt color dependent: experience in a disseminated lymphoma model. *Mol Imaging Biol.* 2021;23:697-702.

14. Teeling JL, French RR, Cragg MS, et al. Characterization of new human CD20 monoclonal antibodies with potent cytolytic activity against non-Hodgkin lymphomas. *Blood.* 2004;104:1793-1800.

15. Repetto-Llamazares AH, Larsen RH, Mollatt C, Lassmann M, Dahle J. Biodistribution and dosimetry of ^{177}Lu-tetulomab, a new radioimmunoconjugate for treatment of non-Hodgkin lymphoma. *Curr Radiopharm.* 2013;6:20-27.

16. ENVIGO. A comparative analysis of Rag2/Il2rg (R2G2) and NSG radiosensitivity. *ENVIGO.* 2017;https://insights.envigo.com/r2g2-radiation-study-data-a-comparative-analysis-of-r2g2-and-nsg-radiosensitivity.

17. Ghetie MA, Richardson J, Tucker T, Jones D, Uhr JW, Vitetta ES. Disseminated or localized growth of a human B-cell tumor (Daudi) in SCID mice. *Int J Cancer.* 1990;45:481-485.

18. Havlena GT, Kapadia NS, Huang P. et al. Cure of micrometastatic B-cell lymphoma in a scid mouse model using ^{213}Bi anti-CD20 monoclonal antibody. *J Nuc Med.* 2022;Epub ahead of print; doi:10.2967/jnumed.122.263962.

19. Bander NH, Milowsky MI, Nanus DM, Kostakoglu L, Vallabhajosula S, Goldsmith SJ. Phase I trial of ^{177}lutetium-labeled J591, a monoclonal antibody to prostate-specific membrane antigen, in patients with androgen-independent prostate cancer. *J Clin Oncol.* 2005;23:4591-4601.

20. Stillebroer AB, Boerman OC, Desar IM, et al. Phase 1 radioimmunotherapy study with lutetium 177-labeled anti-carbonic anhydrase IX monoclonal antibody girentuximab in patients with advanced renal cell carcinoma. *Eur Urol.* 2012;64:478-485.

21. Yadav MP, Singla S, Thakral P, Ballal S, Bal C. Dosimetric analysis of ^{177}Lu-DOTA-rituximab in patients with relapsed/refractory non-Hodgkin's lymphoma. *Nucl Med Commun.* 2016;37:735-742.

22. Giesen D, Lub de Hooge MN, Nijland, M et al. ^{89}Zr-PET imaging to predict tumor uptake of ^{177}Lu-NNV003 anti-CD37 radioimmunotherapy in mouse models of B cell lymphoma. *Sci Rep.* 2022;12:6286.

23. Ertveldt T, De Beck L, De Ridder K, et al. Targeted radionuclide therapy with low and high-dose lutetium-177-labeled single domain antibodies induces distinct

immune signatures in a mouse melanoma model. *Mol Cancer Ther.* 2022;21:1136-1148.

24. Tully KM, Tendler S, Carter LM, et al. Radioimmunotherapy targeting Delta-like ligand 3 in small cell lung cancer exhibits antitumor efficacy with low toxicity. *Clin Cancer Res.* 2022;28:1391-1401.
25. Kostelnik TI, Orvig C. Radioactive main group and rare earth metals for imaging and therapy. *Chem Rev.* 2019;119:902-956.
26. Malenge MM, Patzke S, Ree AH, et al. ^{177}Lu-lilotomab satetraxetan has the potential to counteract resistance to rituximab in non-Hodgkin's lymphoma. *J Nucl Med.* 2020;61:1468-1475.
27. Repetto-Llamazares AHV, Malenge MM, O'Shea A, et al. Combination of ^{177}Lu-lilotomab with rituximab significantly improves the therapeutic outcome in preclinical models of non-Hodgkin's lymphoma. *Eur J Haematol.* 2018;101:522-531.
28. Krasniqi A, D'Huyvetter M, Xavier C, et al. Theranostic radiolabeled anti-CD20 sdAb for targeted radionuclide therapy of non-Hodgkin lymphoma. *Mol Cancer Ther.* 2017;16:2828-2839.
29. Forrer F, Oechslin-Oberholzer C, Campana B, et al. Radioimmunotherapy with ^{177}Lu-DOTA-rituximab: final results of a phase I/II Study in 31 patients with relapsing follicular, mantle cell, and other indolent B-cell lymphomas. *J Nucl Med.* 2013;54:1045-1052.
30. Kumar A, Planchais C, Fronzes R, Mouquet H, Reyes N. Binding mechanisms of therapeutic antibodies to human CD20. *Science.* 2020;369:793-799.

31. Beyer G-J, Miederer M, Vranješ-Đurić S, et al. Targeted alpha therapy in vivo: direct evidence for single cancer cell kill using ^{149}Tb-rituximab. *Eur J Nucl Med Mol Imaging.* 2004;31:547-54.

32. Green DJ, Shadman M, Jones JC, et al. Astatine-211 conjugated to an anti-CD20 monoclonal antibody eradicates disseminated B-cell lymphoma in a mouse model. *Blood.* 2015;125:2111-2119.

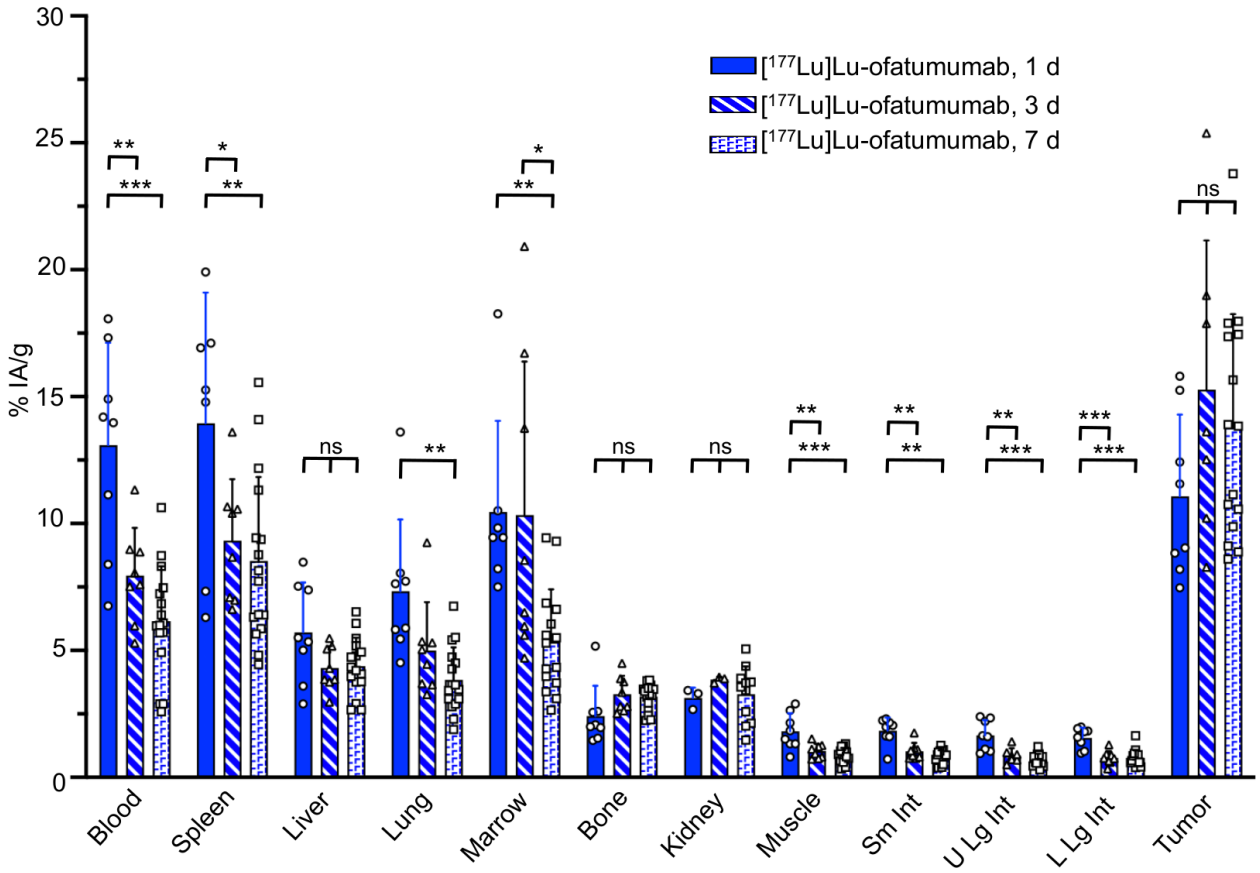

FIGURE 1. [^{177}Lu]Lu-ofatumumab biodistribution in R2G2 mice with subcutaneous Raji tumors. Biodistribution was assayed 1, 3 or 7 post-radiopharmaceutical injection (n=3-16 mice/time point) with data presented as mean±standard deviation. One-way ANOVA comparing the distribution in an organ/tissue at each time point. *, p<0.05, **, p<0.001, ***, p<0.0001. Sm Int, small intestine. U Lg Int, upper large intestine. L Lg Int, lower large intestine.

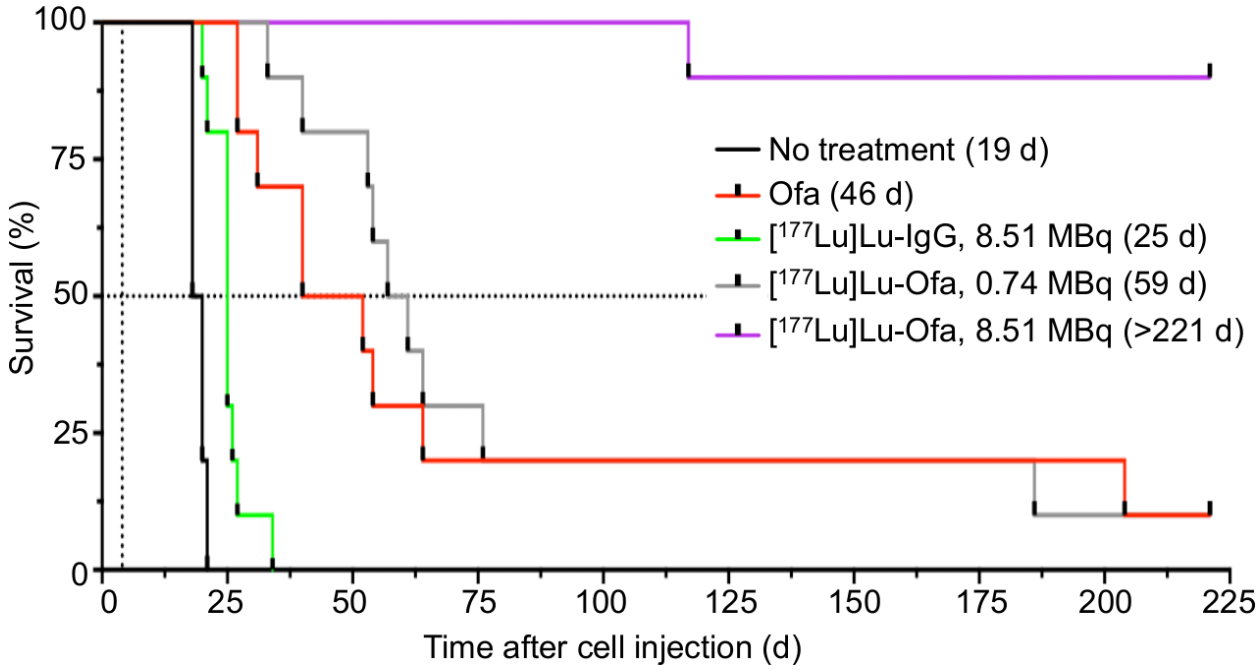

FIGURE 2. Survival analysis of mice with disseminated Raji-luc cells with therapy initiated 4 d post cell injection. Kaplan-Meier graph with median survival indicated in days. Ofa, ofatumumab.

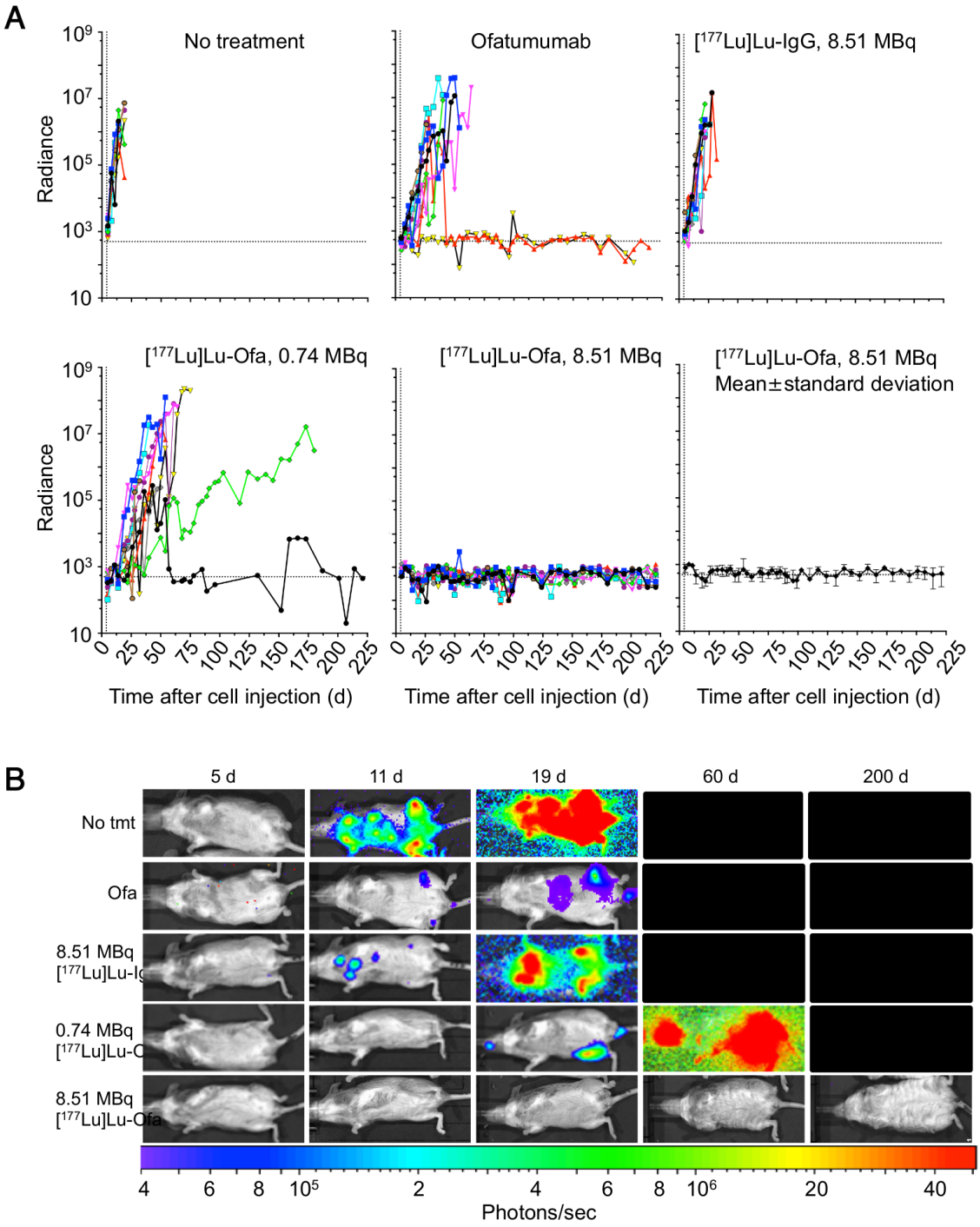

FIGURE 3. Tumor burden of mice with disseminated Raji-luc cells with therapy initiated 4 d post cell injection. (A) Bioluminescence, n=10 mice/group. (B) Representative bioluminescence images at the indicated d post-cell injection. Radiance, (photons/sec/cm^2/steradian). Ofa, ofatumumab.

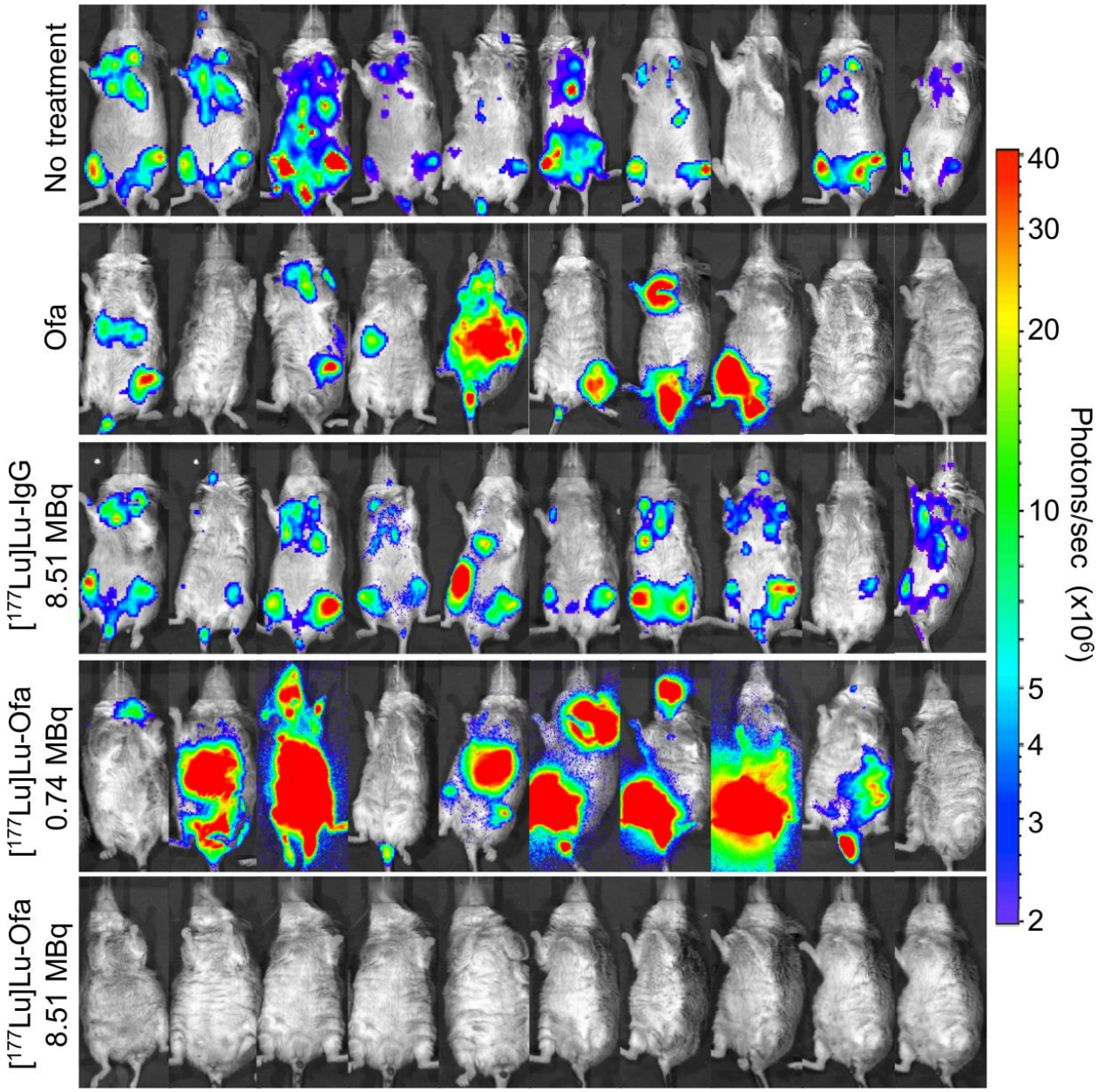

FIGURE 4. Bioluminescence images of untreated or treated mice with disseminated Raji-luc cells on the final imaging event prior to sacrifice for cause or study termination. Ofa, ofatumumab.

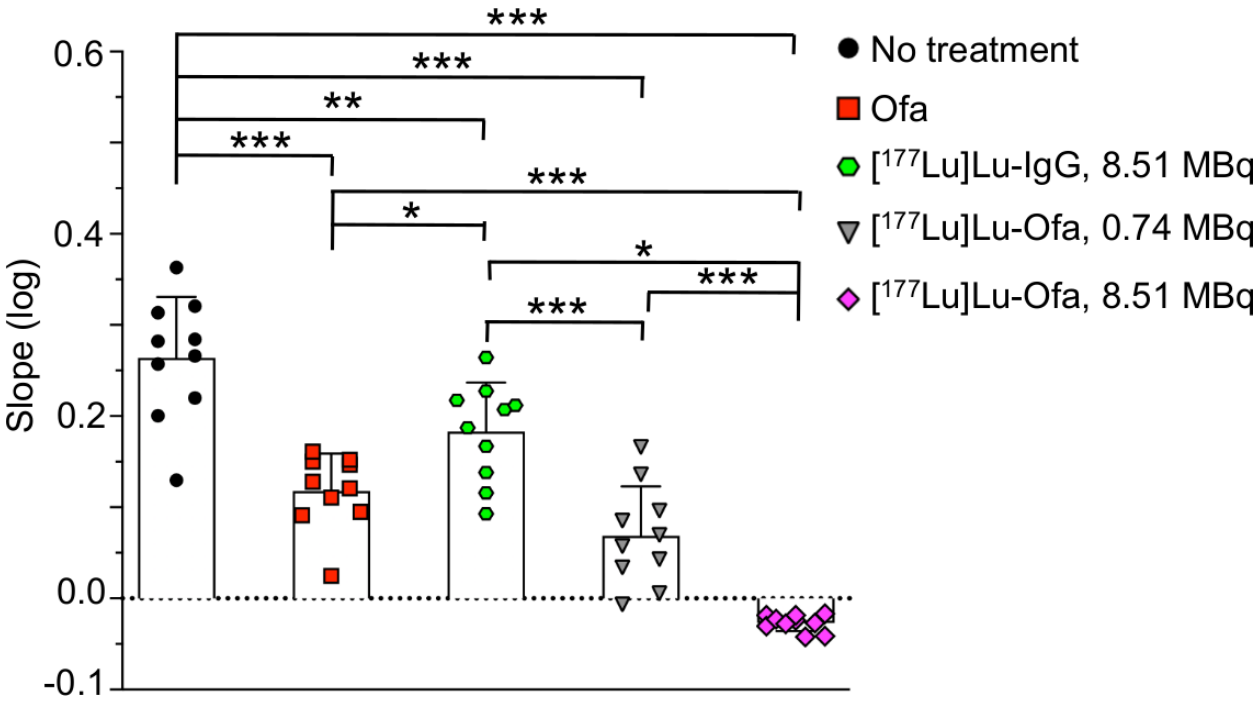

FIGURE 5. Tumor-cell growth in mice one to eighteen d post initiation of therapy. Log of the slopes of the radiance (photons/sec/cm^2/steradian) over this time are shown as mean±standard deviation and were analyzed by ANOVA, comparing all samples with each other, n=10 mice/group. *, p<0.05, ** p<0.005, ***, p<0.0001. Ofa, ofatumumab.

Graphical Abstract

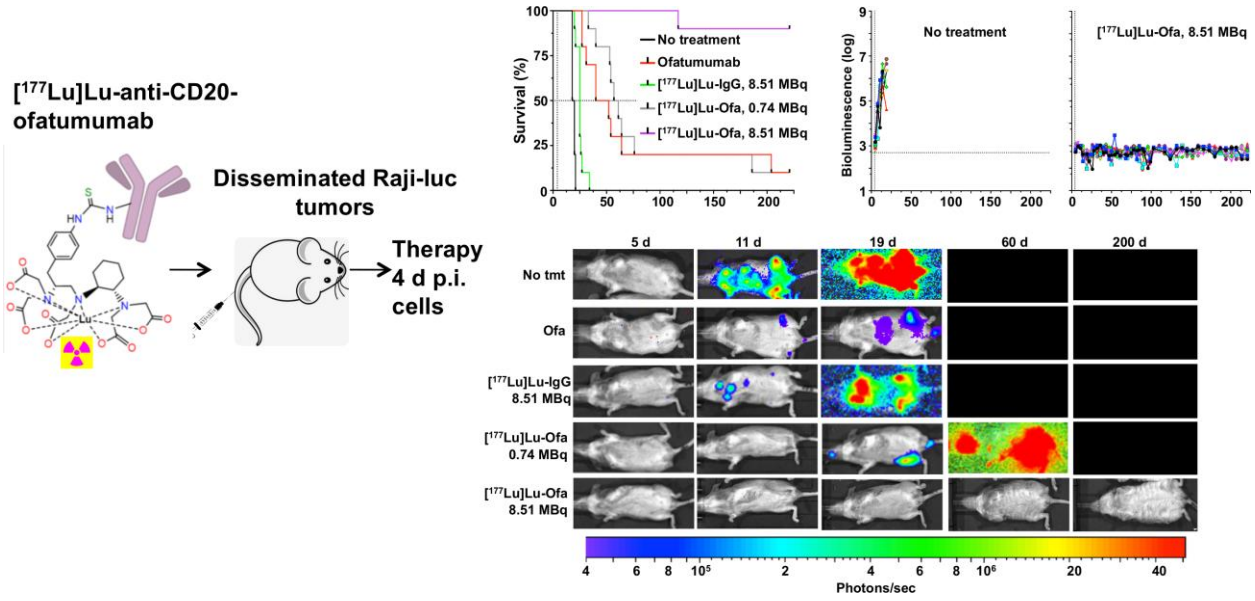

TABLE 1
Human radiation dose estimates for [^{177}Lu]Lu-ofatumumab extrapolated to the adult female model

Organ	mSv/MBq (rad/mCi)
Adrenals	0.39 (1.44)
Brain	0.05 (0.19)
Breasts	0.25 (0.91
Esophagus	0.26 (0.96)
Eyes	0.25 (0.91)
Gallbladder wall	0.28 (1.02)
Left colon	0.36 (1.34)
Small Intestine	0.41 (1.50)
Stomach wall	0.29 (1.09)
Right colon	0.29 (1.08)
Rectum	0.26 (0.97
Heart wall	1.02 (3.77)
Kidneys	0.43 (1.60)
Liver	0.36 (1.32)
Lungs	0.53 (1.96)
Ovaries	0.39 (1.44)
Pancreas	0.21 (0.77)
Salivary glands	0.25 (0.92)
Red marrow	0.54 (2.01)
Osteogenic cells	0.82 (3.02)
Spleen	0.48 (1.76)
Thymus	0.26 (0.96)
Thyroid	0.80 (2.97)
Urinary bladder wall	0.34 (1.27)
Uterus	0.54 (2.00)
Total body	0.31 (1.14)
Effective dose (mGy/MBq; rem/mCi)	0.36 (1.34)

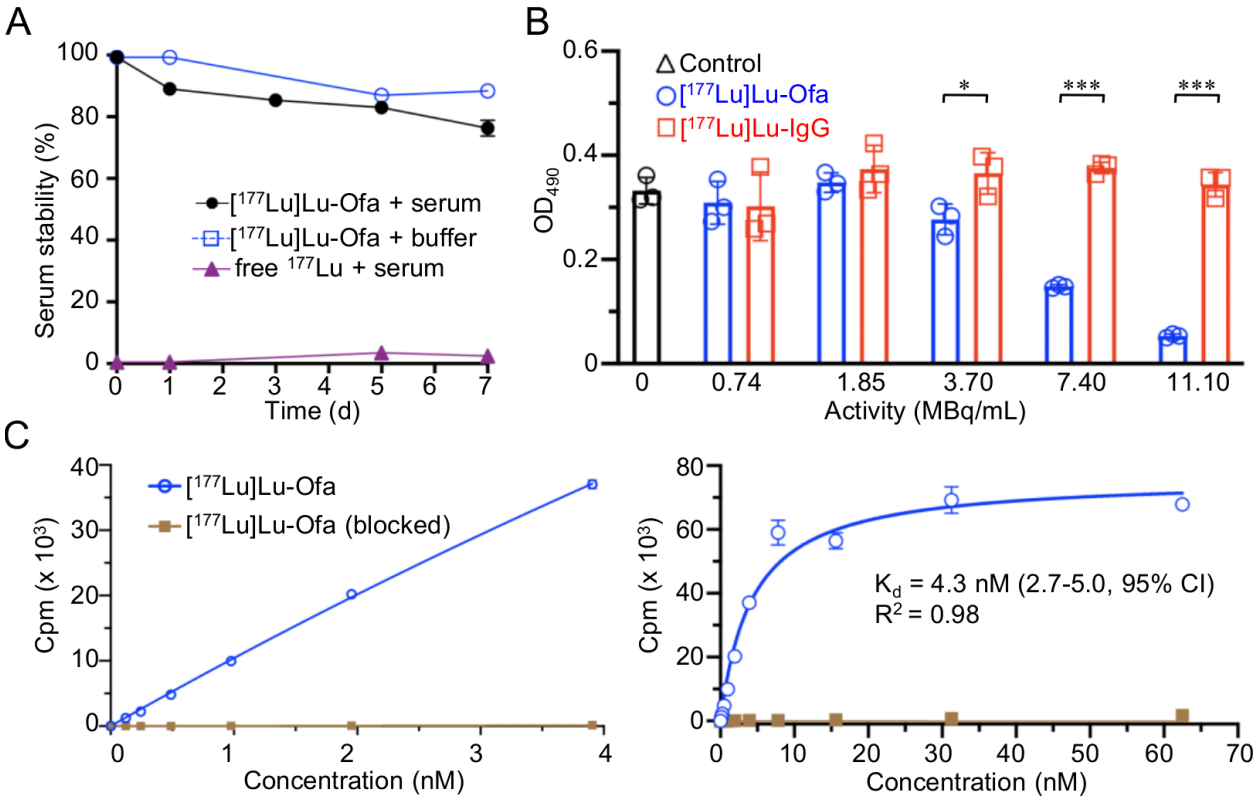

SUPPLEMENTAL FIGURE 1. [^{177}Lu]Lu-ofatumumab in vitro stability, cell killing and affinity. (A) Stability in serum at 37˚C and buffer at 4˚C (n=3). (B) Killing of Raji-luc cells (n=3). Student's unpaired *t*-test, comparing [^{177}Lu]Lu-ofatumumab and [^{177}Lu]Lu-IgG. *, $p<0.05$, ***, $p<0.0001$. (C) Raji-cell saturation binding assay shown at two scales, with or without blocking (n=3). Cpm, counts per minute. Ofa, ofatumumab.

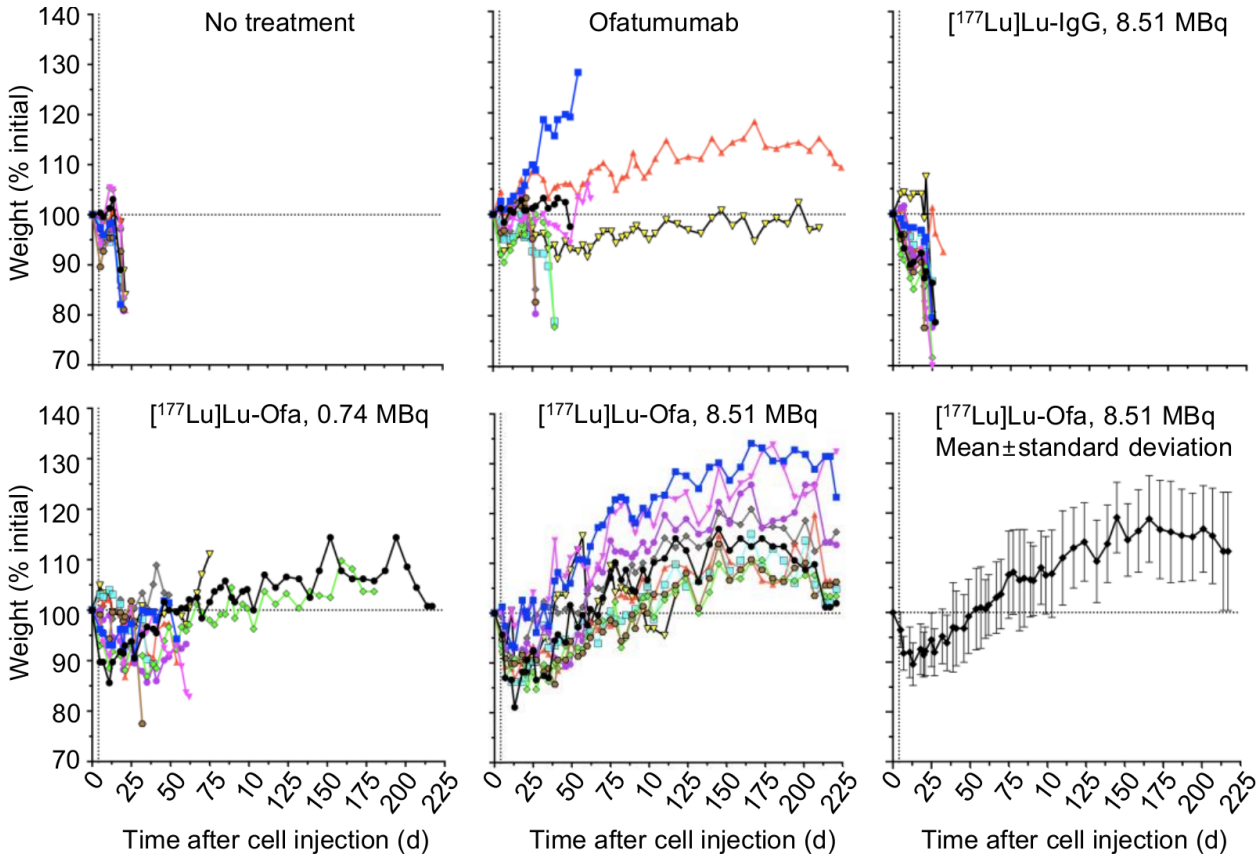

SUPPLEMENTAL FIGURE 2. Weights of mice with disseminated Raji-luc cells with therapy initiated 4 d post cell injection. ANOVA tests of 8.51 MBq [^{177}Lu]Lu-ofatumumab treated mice, comparing to d 0 weights, indicated weight loss from 10 d to 35 d and weight gain after 75 d (p<0.05). n=10 mice/group. Ofa, ofatumumab.

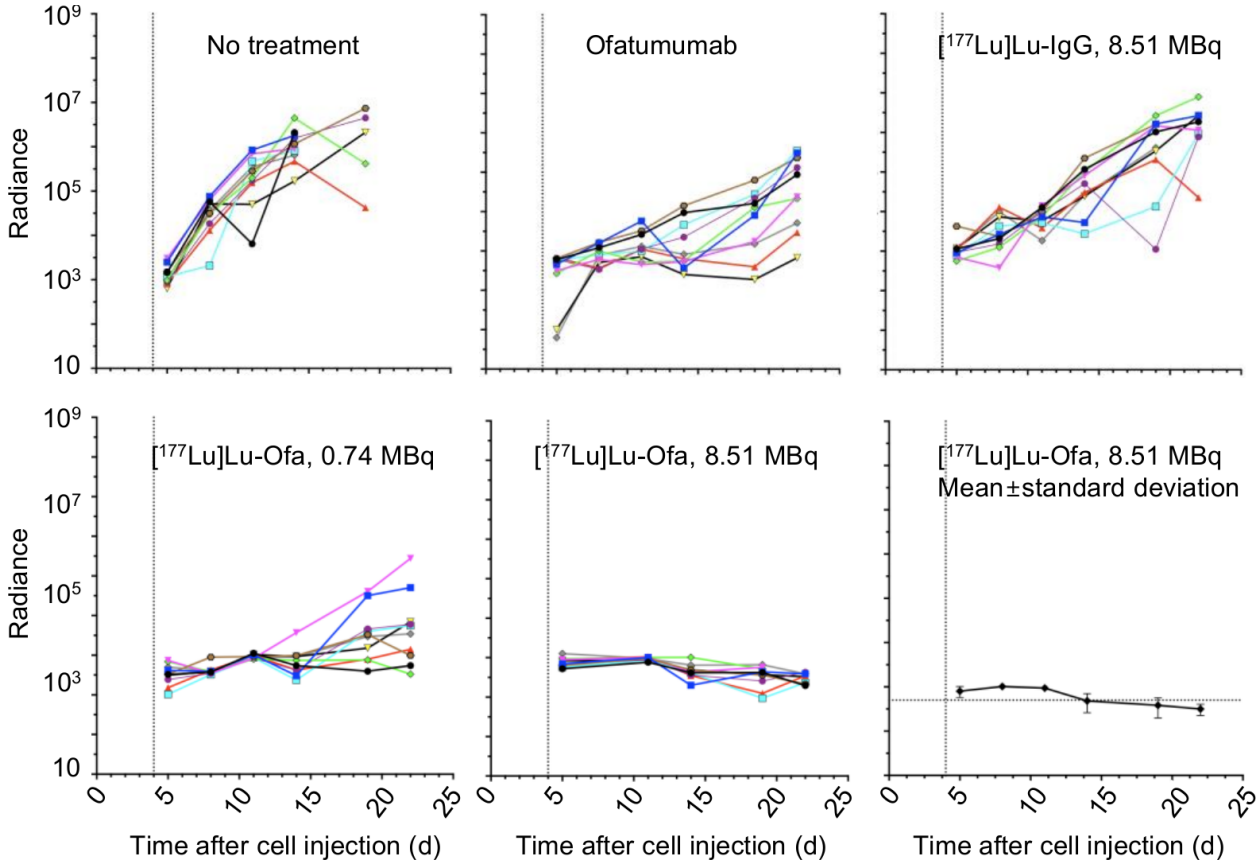

SUPPLEMENTAL FIGURE 3. Tumor-cell growth in mice one to eighteen d post initiation of therapy. Radiance (photons/sec/cm^2/steradian) values of individual mice and the mean±standard deviation of mice treated with 8.51 MBq of [^{177}Lu]Lu-ofatumumab are shown. Ofa, ofatumumab.

SUPPLEMENTAL TABLE 1

Biodistribution (% IA/g) of [^{177}Lu]Lu-ofatumumab in C57Bl/6N mice

[^{177}Lu]Lu-ofatumumab	4 h	1 d	2 d	7 d	11 d
Blood	37.63 ± 7.76	26.57 ± 1.76	31.04 ± 2.24	23.37 ± 4.04	19.22 ± 2.77
Heart	10.18 ± 3.12	7.6 ± 1.81	8.22 ± 1.76	6.24 ± 1.14	5.37 ± 1.32
Liver	9.07 ± 1.88	6.36 ± 0.50	6.89 ± 0.98	5.96 ± 0.93	5.30 ± 0.72
Bone	3.32 ± 0.73	3.59 ± .29	3.31 ± 0.49	3.81 ± 0.37	3.36 ± 0.41
Marrow	13.88 ± 2.26	12.20 ± 1.55	14.84 ± 3.91	9.63 ± 1.18	8.59 ±1.23
Spleen	9.03 ± 1.71	8.30 ± 0.87	9.66 ± 1.38	8.18 ± 1.74	7.89 ± 1.45
Kidney	9.56 ± 1.84	7.59 ± 0.24	9.32 ± 1.20	7.95 ± 1.11	5.92 ± 0.45
Bladder	4.99 ± 0.98	8.17 ± 1.23	9.18 ± 1.06	6.86 ± 1.06	6.84 ± 1.46
Lung	13.06 ± 2.52	10.23 ± 0.79	12.46 ± 1.15	8.97 ± 1.25	7.38 ± 0.97
Gallbladder	3.06 ± 1.29	2.49 ± 0.98	3.27 ± 1.82	3.30 ± 2.05	5.74 ± 2.83
Muscle	2.37 ± 0.50	4.27 ± 0.22	4.89 ± 0.50	3.20 ± 0.30	2.55 ± 0.21
Fat	3.19 ± 1.10	5.08 ± 1.15	3.92 ± 036	2.47 ± 0.86	2.35 ± 0.74
Brain	1.03 ± 0.44	0.77 ± 0.04	0.98 ± 0.31	0.74 ± 0.09	0.58 ± 0.15
Uterus	10.72 ± 8.98	10.50 ± 1.64	10.13 ± 1.78	9.07 ±2.72	8.64 ± 3.90
Ovaries	6.00 ± 1.44	8.23 ± 0.72	8.02 ± 1.98	4.36 ± 1.13	4.53 ± 1.47
Adrenals	10.61 ± 2.57	9.04 ± 2.00	8.31 ± 3.74	6.49 ± 1.07	6.31 ± 1.67
Thyroid	6.82 ± 0.87	6.91 ± 2.06	7.70 ± 2.07	6.87 ± 1.51	4.69 ± 0.55
Pancreas	3.73 ± 0.96	5.21 ± 0.62	4.05 ± 0.52	3.20 ± 0.43	2.59 ± 0.43
Thymus	4.14 ± 1.59	4.12 ± 0..32	5.66 ± 1.68	3.97 ± 0.48	2.74 ± 0.56
Stomach	2.66 ± 0.60	2.34 ± 0.62	3.21 ± 0.62	2.13 ± 0.80	1.64 ± 0.79
Sm Int	4.21 ± 0.93	3.05 ± 0.47	3.73 ± 0.42	2.51 ± 0.50	1.89 ± 0.34
U Lg Int	4.02 ± 0.41	2.94 ± 0.27	4.12 ± 0.34	2.43 ± 0.55	1.71 ± 0.49
L Lg Int	2.81 ± 0.36	2.07 ± 0.09	2.55 ± 0.43	1.89 ± 0.32	1.37 ± 0.18

Values represent %IA/g±SD, except for urine and feces, which were collected as a pooled sample. n=5 mice/time point. Sm Int, small intestine. U Lg Int, upper large intestine. L Lg Int, lower large intestine.

SUPPLEMENTAL TABLE 2

Integrated time-activity for [^{177}Lu]Lu-ofatumumab extrapolated to humans

Organ/Tissue	Integrated time activity (h)
Blood	59.70
Lung	5.57
Liver	5.31
Spleen	0.68
Kidney	1.30
Bladder	0.17
Gallbladder	0.02
Muscle	39.17
Fat	15.92
Heart	1.04
Brain	0.59
Bone (surfaces)	9.26
Red marrow	5.86
Uterus	0.47
Ovaries	0.04
Adrenals	0.05
Thyroid	0.16
Pancreas	0.25
Thymus	0.05
Stomach	0.19
Small Int	0.96
U Lg Int	0.13
L Lg Int	0.18
Heart content	5.37
Bladder content	0.31
Excreted	31.70
Remainder of body	121.33

Analysis of C57Bl/6N mice. Bladder content was estimated using the excretion data and MIRD voiding bladder model assuming 3.2 h void interval. Sm Int, small intestine. U Lg Int, upper large intestine. L L Int, lower large intestine.

SUPPLEMENTAL TABLE 3

Phenotypes associated with death/sacrifice

	HLP	W	O	Sur
No treatment	10	0	0	0
Ofa	7	1	1	1
[^{177}Lu]Lu-IgG, 8.51 MBq	10	0	0	0
[^{177}Lu]Lu-Ofa, 0.74 MBq	7	1	1	1
[^{177}Lu]Lu-Ofa, 8.51 MBq	0	0	1	9

Phenotypes associated with death/sacrifice in therapy study of initiated 4 d post-cell injection. n=10 mice/group. HLP, hind-limb paralysis. W, loss of >20% of initial weight. O, event other than HLP or weight loss. Ofa, ofatumumab. Sur, survival.